

Xenotransplantation elicits salient tumorigenicity of adult T-cell leukemia-derived cells via aberrant AKT activation

Kazunori Yamaguchi,^{1,2} Tomoka Takanashi,¹ Kentaro Nasu,^{1,3} Keiichi Tamai,^{2,4} Mai Mochizuki,^{1,2} Ikuro Satoh,^{2,5} Shoji Ine,⁶ Osamu Sasaki,⁶ Kennichi Satoh,^{2,7} Nobuyuki Tanaka,^{2,4} Hideo Harigae³ and Kazuo Sugamura¹

¹Division of Molecular and Cellular Oncology, Miyagi Cancer Center Research Institute, Natori; ²Departments of ²Cancer Science; ³Hematology and Rheumatology, Tohoku University Graduate School of Medicine, Sendai; ⁴Division of Cancer Biology and Therapeutics, Miyagi Cancer Center Research Institute, Natori; ⁵Departments of ⁵Pathology; ⁶Hematology, Miyagi Cancer Center, Natori; ⁷Division of Cancer Stem Cells, Miyagi Cancer Center Research Institute, Natori, Japan

Key words

Adult T-cell leukemia, proto-oncogene protein Akt, severe combined immunodeficient mice, tumor-initiating cells, xenotransplantation

Correspondence

Kazuo Sugamura, 47-1 Nodayama, Medeshima-Shiode, 981-1293 Natori, Miyagi, Japan.
Tel: +81-22-384-3151; Fax: +81-22-381-1195;
E-mail: sugamura@med.tohoku.ac.jp

Funding Information

Japan Society for the Promotion of Science (KAKENHI/24570142, KAKENHI/25290047, KAKENHI/26830087).

Received December 8, 2015; Revised February 13, 2016;
Accepted February 23, 2016

Cancer Sci 107 (2016) 638–643

doi: 10.1111/cas.12921

Adult T-cell leukemia/lymphoma (ATL) is a life-threatening hematologic malignancy triggered by the human retrovirus HTLV-1.⁽¹⁾ Although the viral oncogenes *Tax* and *HBZ* are thought to play critical roles in the development of ATL,^(2–4) additional cellular events, such as gene mutation, aberrant gene expression, or deregulated signal transduction, are thought to take place for several decades after the initial HTLV-1 infection.⁽⁵⁾ However, these later ATL-associated events have not been elucidated.

The heterogeneity of tumor cells is a long-standing concept that was first discovered by pathological observations,^(6,7) and was more recently supported by molecular-level analyses.⁽⁸⁾ There is increasing evidence that cellular heterogeneity exists in many types of cancers, including leukemia and even in cultured tumor cells *in vitro*. Working on the assumption that ATL cells possess cellular heterogeneity, we sought to identify highly tumorigenic cell populations from ATL-derived cell lines. Given that the tumorigenicity of human cancer cells is often evaluated by their xenotransplantability in immunodeficient mice,⁽⁹⁾ we previously established immunodeficient NOG mice, which are useful for identifying cancer stem cell-like populations of human cancers⁽¹⁰⁾ and, using these mice, we and others have identified cancer stem cell-like populations of human liver cancer,⁽¹¹⁾ hypopharyngeal cancer,⁽¹²⁾ cholangiocarcinoma,⁽¹³⁾ and colon carcinoma⁽¹⁴⁾ cells.

The transplantation of human cancer cells into immunodeficient NOD/SCID/IL-2R γ ^{null} (NOG) mice often causes highly malignant cell populations like cancer stem cells to emerge. Here, by serial transplantation in NOG mice, we established two highly tumorigenic adult T-cell leukemia-derived cell lines, ST1-N6 and TL-Om1-N8. When transplanted *s.c.*, these cells formed tumors significantly earlier and from fewer initial cells than their parental lines ST1 and TL-Om1. We found that protein kinase B (AKT) signaling was upregulated in ST1-N6 and TL-Om1-N8 cells, and that this upregulation was due to the decreased expression of a negative regulator, INPP5D. Furthermore, the introduction of a constitutively active AKT mutant expression vector into ST1 cells augmented the tumorigenicity of the cells, whereas treatment with the AKT inhibitor MK-2206 attenuated the progression of tumors induced by ST1-N6 cells. Collectively, our results reveal that the AKT signaling pathway plays a critical role in the malignancy of adult T-cell leukemia-derived cells.

In this study, we obtained highly tumorigenic populations of ATL-derived ST1 and TL-Om1 cells after their serial transplantation into NOG mice. These cell populations showed evidence of an activated AKT signaling pathway, which may contribute to the malignancy observed in the ATL-derived cells.

Materials and Methods

Reagents. All chemicals were purchased from Wako (Osaka, Japan) unless otherwise specified. The antibodies against PTEN, AKT, phosphorylated AKT (T308, S473), FOXO1, FOXO3a, phosphorylated FOXO1 (T24), phosphorylated FOXO3a (T32), and INPP5D were purchased from Cell Signaling Technology (Danvers, MA, USA). The HRP-conjugated anti-tubulin antibody was purchased from MBL (Nagoya, Japan). The anti-HA antibody was purchased from Roche (Mannheim, Germany). The plasmid DNAs pLNCX-Myr-HA-Akt (plasmid #9005; Addgene, Cambridge, MA, USA)⁽¹⁵⁾ and p1242 3-KB-L (plasmid #26699; Addgene)⁽¹⁶⁾ were kind gifts from Dr. W. Sellers (Harvard Medical School, Boston, MA, USA) and Dr. B. Sugden (University of Wisconsin, Madison, WI, USA), respectively.

Cell culture and serial transplantation. NOG⁽¹⁰⁾ mice were supplied by the Central Institute for Experimental Animals

(Kawasaki, Japan) and were used for experiments after a 1-week acclimation period. The mice were kept at 25°C on a 12:12-h light : dark cycle and were provided with laboratory chow and water *ad libitum*. The protocols for all animal experiments were approved by the Miyagi Cancer Center Animal Care and Use Committee (permission number: MCC-AE-2011-1).

The ATL-derived cell line ST1 was a kind gift from Dr. Yamada (Nagasaki University, Nagasaki, Japan).⁽¹⁷⁾ The TL-Om1 cell line had been established previously.⁽¹⁸⁾ Both were maintained in RPMI medium supplemented with 10% FBS (Gibco, Grand Island, NY, USA) and penicillin/streptomycin under 5% CO₂ at 37°C in humidified conditions. To induce tumors, the cells were suspended in RPMI medium, mixed with an equal volume of Matrigel (BD Biosciences, Bedford, MA, USA),⁽¹⁹⁾ and s.c. injected into the back of NOG mice (8–10 weeks old). The mice were observed every day for morbidity, and tumor development was assessed by measuring the tumor length and width using a caliper.

For serial transplantation, the developed tumors were dissected and minced with scissors in RPMI medium followed by incubation with Collagenase/Dispase and DNase I (both from Roche Diagnostics) at 37°C for 1 h. Cells were liberated from the tumors by pipetting, and the resulting cell suspension was filtered through a 70- μ m cell strainer (BD Falcon, Franklin Lakes, NJ, USA). To avoid collecting a biased cell population originating from mouse-to-mouse or tumor-to-tumor variation, we pooled all of the cells prepared from each tumor from all of the injected mice (two to three mice for each serial injection step) and used the pooled cells for the subsequent xenotransplantation or experiments. Cells were seeded in culture medium and cultured for 1 week prior to the next injection. For experiments using the AKT inhibitor MK-2206 (Cayman Chemical, Ann Arbor, MI, USA), the MK-2206 was first dissolved in 30% Captisol (ChemScene, Monmouth Junction, NJ, USA) and then i.p. injected (100 mg/kg) twice a week.⁽²⁰⁾

To evaluate the plating efficiency of the ST1 and ST1-N6 cells *in vitro*, the cells were stained with 7-aminoactinomycin D to eliminate dead cells and sorted by FACS Aria (BD Biosciences) to deliver a single cell per well into 96-well plates. Each well contained 200 μ L RPMI medium supplemented with 10% FBS (Gibco) and penicillin and streptomycin. The sorted cells were cultured under 5% CO₂ at 37°C in humidified conditions for 1 week, and then examined under a microscope. The number of wells containing more than 10 cells was counted.

Construction of a plasmid vector. To construct an expression vector for HA-tagged CA-AKT, the insert sequence of pLNCX-Myr-HA-Akt (Addgene) was amplified using KOD FX polymerase (Toyobo, Osaka, Japan) following the manufacturer's recommendation, with primers 5'-CTGAATTCCAC-CATGGGGTCTTCAAATCTAAAC-3' and 5'-CTGAATTCTCAGGCCGTGCCGCTGGCCGAGT-3' and subcloned into the *Eco*RI site of the pRetroX-Tight-Pur retrovirus vector (Clontech, Palo Alto, CA, USA) using a ligation kit (TaKaRa Bio, Ohtsu, Japan).

Transduction of cells. Retrovirus was generated with a packaging cell Plat A (a generous gift from Dr. T. Kitamura, Tokyo University, Tokyo, Japan). Plasmid DNA of the retrovirus vector was transferred using FuGENE HD (Promega, Madison, WI, USA) into Plat A cells following the manufacturer's recommendation. The culture medium was harvested 48 h after transfection and filtered through a 0.45- μ m filter (Kurabo, Tokyo, Japan). It was then used for the transduction

of ST1 cells, which was achieved by spinfection (1500 g, 2 h, 37°C). To obtain cells expressing CA-AKT, ST1 cells were first transduced with a pRetroX-Tet-On Advanced retrovirus vector (Clontech) by spinfection and selected by G418 (1 mg/mL). The G418-resistant cells were then used for additional transduction with a CA-AKT-coding pRetroX-Tight-Pur retrovirus. Cells were selected with culture medium containing 0.5 μ g/mL puromycin plus 1 mg/mL G418.

Western blot analysis. Cells (5×10^6) were washed once with PBS(-) and sonicated in cold lysis buffer (50 mM HEPES [pH 7.5], 150 mM NaCl, 1% Triton X-100, 2 mM EDTA, 10 mM NaF, 2 mM sodium orthovanadate, 2 mM phenylmethylsulfonyl fluoride, 7.5 μ g/mL aprotinin, and 10 μ g/mL leupeptin) for 5 min. The lysates were clarified by brief centrifugation (10 000 g), and the supernatant was used for analysis. To prepare protein samples from tumors, the dissected tumor was rinsed in PBS(-) and homogenized in the cold lysis buffer using an MM300 (Qiagen, Valencia, CA, USA) according to the manufacturer's recommendation. After measuring the protein concentration with a protein assay kit (Bio-Rad Laboratories, Richmond, CA, USA), the sample (10 μ g protein) was mixed with an equal volume of SDS-loading buffer (100 mM Tris-Cl [pH 6.8], 4% SDS, 0.2% bromophenol blue, 20% glycerol, and 2% β -mercaptoethanol), boiled for 5 min, and separated by electrophoresis through SDS polyacrylamide gel (Wako). The separated proteins were transferred onto a PVDF membrane (Millipore, Billerica, MA, USA), which was incubated with 1/1000-diluted primary antibody and then with HRP-conjugated anti-mouse, anti-goat, or anti-rabbit antibody (Santa Cruz Biotechnology, Santa Cruz, CA, USA) as recommended by the manufacturers. Primary antibody binding was detected using a West Pico chemiluminescent kit (Pierce, Rockford, IL, USA) and a camera with a charge-coupled device (Fuji Film, Tokyo, Japan).

Polymerase chain reaction. RNA was prepared from cells with an RNeasy mini kit (Qiagen) and then reverse-transcribed into cDNA with PrimeScript (TaKaRa Bio) following the manufacturers' instructions. Gene expression was assessed by real-time PCR with a Brilliant assay kit (Agilent Technologies, Santa Clara, CA, USA) and LC480 (Roche Diagnostics). The primer sequences used are listed in Table S1.

Gene knock-down by siRNA. For siRNA-mediated gene knock-down, siRNAs were designed with siDirect (<http://sidiirect2.rnai.jp/>) and synthesized by FASMAC (Atsugi, Japan). The siRNA sequences used are listed in Table S1. The siRNA was introduced by electroporation (CUY21; Neppagene, Ichikawa, Japan) under conditions recommended by the manufacturer.

Statistics. Most of the experiments were carried out at least three times, and the data were evaluated using Student's *t*-test.

Results

Serial transplantation upregulates tumorigenicity of ATL-derived cell lines. To investigate the molecular mechanisms underlying the tumorigenicity of ATL cells, we sought to obtain highly tumorigenic sublines from ATL-derived cell lines. To this end, we serially transplanted the ATL-derived ST1 cells into immunodeficient NOG mice. Cells that had passed through six rounds of xenotransplantation (hereafter called ST1-N6 subline cells) formed tumors earlier than did the parental ST1 cells (Figs 1a,S1). Limiting dilution analyses revealed that tumors developed from smaller initial numbers of ST1-N6 cells than ST1 cells (Fig. 1b). These results suggested

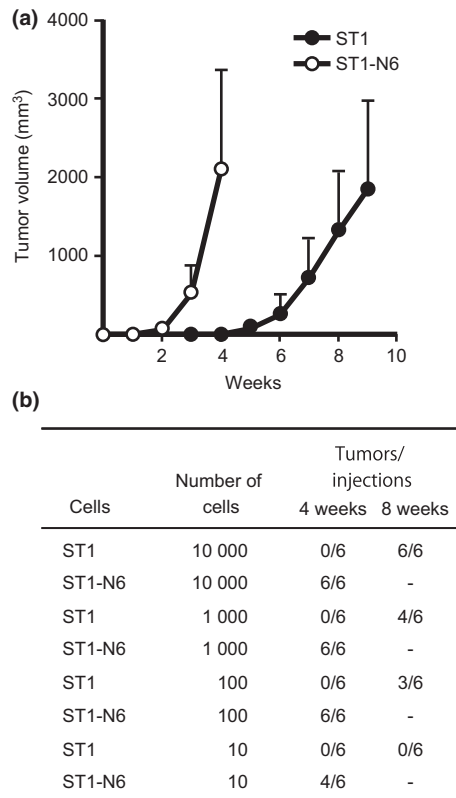


Fig. 1. Increased tumorigenicity of adult T-cell leukemia/lymphoma-derived cell lines by serial transplantation. (a) Tumor growth of ST1 and ST1-N6 cells in NOG mice. After cell injection (10^4 cells/site), the sizes of the developed tumors were measured by a caliper and tumor volumes were plotted. To calculate tumor volume, the modified ellipsoid formula, $1/2(\text{length} \times \text{width}^2)$, was used. Results from six injection sites were averaged. (b) Limiting dilution analysis of tumor development. Different numbers of ST1 or ST1-N6 cells were injected, and the number of tumors at 4 and 8 weeks post-injection per total number of injection sites was determined. Mice were sacrificed once a tumor exceeded 20 mm in diameter, which occurred before 8 weeks post-injection in the ST1-N6-treated animals (indicated by -).

that the ST1-N6 cells were more tumorigenic, with more robust tumor-initiating activity, compared with the parental ST1 cells. We also obtained a highly tumorigenic subline, TL-Om1-N8, from another ATL-derived cell line, TL-Om1, which had passed through eight rounds of xenotransplantation in NOG mice (Fig. S2). Taken together, these results indicated that serial transplantation in NOG mice is a useful approach for establishing highly tumorigenic sublines from ATL-derived cell lines such as ST1 and TL-Om1.

To address whether the high tumorigenicity of the ST1-N6 and TL-Om1-N8 cells correlated with their *in vitro* growth properties, we measured their growth rates and plating efficiencies *in vitro*. There was no difference in the growth rate between the parental ST1 and ST1-N6 cells, or between the TL-Om1 and TL-Om1-N8 cells (Fig. S3a,b). To assess plating efficiencies, cells were seeded into 96-well culture plates at 1 cell per well using a cell sorter, and 1 week after seeding, the number of wells containing more than 10 cells was counted. No significant difference between the ST1 and ST1-N6 cells was observed in the number of wells in which cells had proliferated from a single cell (Fig. S3c). These results suggested that the high tumorigenicity of ST1-N6 and TL-Om1-N8 cells was not solely due to the *in vitro* growth properties of these cells.

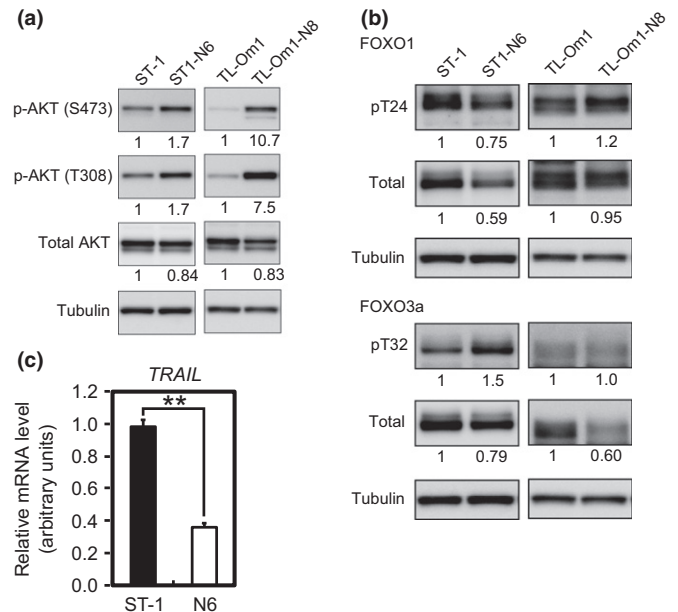


Fig. 2. Upregulation of protein kinase B (AKT) signaling in ST1-N6 cells. (a) Increased phosphorylation of AKT after serial transplantation. Cell lysates were prepared from each cell population and analyzed by Western blotting. Detection of α -tubulin was used as a protein loading control. Band intensities were normalized to the intensity of α -tubulin and then divided by the normalized intensity of the band in the parental ST1 cells. Representative results of three independent experiments are shown. (b) Western blot analysis of FOXO phosphorylation levels. Representative results of three independent experiments are shown. (c) mRNA level of the FOXO-target gene *TRAIL* in ST1 and ST1-N6 cells. The mRNA level was measured by real-time RT-PCR. Results from three independent samples were averaged and are presented with SD. $**P < 0.01$.

Upregulation of AKT signaling in ST1-N6 cells. We next examined which molecular mechanism(s) was responsible for the increased tumorigenicity of the ST1-N6 and TL-Om1-N8 cells. First, we measured the expression levels of *Tax* and *HBZ*, oncogenic genes of HTLV-1, and found that they were rather suppressed in ST1-N6 cells (Fig. S4a). This result infers a minimal relationship between these viral oncogenes and the tumorigenicity of ST1-N6 cells, although this relationship remains to be clarified. We then examined intracellular signaling molecules, and found that the AKT (Fig. 2) and NF- κ B (Fig. S4b) signaling pathways were activated in the ST1-N6 cells. In this paper, we focused on the AKT signaling pathway.

We assessed the phosphorylation states of AKT at T308 and S473, both of which are known to be phosphorylated in response to signals such as growth stimuli, and to be critical for the kinase activity of AKT.⁽²¹⁾ T308 and S473 of AKT were more highly phosphorylated in the ST1-N6 cells than in the parental ST1 cells, although the total amount of AKT protein was slightly decreased in the ST1-N6 cells (Fig. 2a), suggesting that AKT signaling was upregulated in the ST1-N6 cells. The upregulation of AKT was observed in the cells after a single xenotransplantation, and became more pronounced after the fourth xenotransplantation (Fig. S4c).

Concomitant with the AKT upregulation in ST1-N6 cells, FOXO3, a transcription factor that is known to be an AKT substrate and downstream component of AKT signaling, showed a higher phosphorylation rate and lower protein level in ST1-N6 cells than in ST1 cells (Fig. 2b). FOXO3 is phosphorylated on T32 by AKT, which leads to its association with

14-3-3 protein and its subsequent cytoplasmic retention and proteasomal degradation.⁽²²⁾ TL-Om1-N8 cells also showed the downregulation of FOXO3. We detected the T32-phosphorylated form of FOXO3 in TL-Om1-N8 cells, although its level was lower than that in ST1-N6 cells. The level of T32-phosphorylated FOXO3 was not very different between the parental TL-Om1 and TL-Om1-N8 cells, but the protein level was significantly decreased in the latter cells, suggesting that the T32-phosphorylation rate was higher in the TL-Om1-N8 cells. We also found a decreased protein level and increased proportion of T24-phosphorylated FOXO1, another downstream target of the AKT signaling pathway, in ST-N6 cells, although the differences were not as marked as those of FOXO3. In TL-Om1-N8 cells, we observed the increased T24-phosphorylation but no significant decrease in the FOXO1 protein. Consistent with the FOXO downregulation by AKT activation, the expression level of the FOXO target gene *TRAIL* was lower in ST1-N6 than in ST1 cells (Fig. 2c). Taken together, these results indicated that the AKT signaling pathway is constitutively upregulated in ST1-N6 and TL-Om1-N8 cells, suggesting that AKT activation may be involved in the tumorigenicity of ATL-derived cells.

To examine whether or not AKT activation was responsible for the high tumorigenicity of the ST1-N6 cells, we transduced ST1 cells with a tetracycline-regulated retrovirus expression vector encoding the constitutively active form of AKT (CA-AKT). CA-AKT contains the N-terminal myristoylation site of src protein, which enables AKT to bind to the cell membrane and be activated even without PI3K. We found that the transduced cells expressed a detectable level of CA-AKT even without doxycycline induction (Fig. 3a). This “leaky” expression of CA-AKT persisted after tumor development in NOG mice (Fig. 3b). The exogenously expressed CA-AKT was highly phosphorylated, indicating that AKT signaling was constitutively upregulated in the ST1 cells transduced with CA-AKT. This finding was supported by the phosphorylation of FOXO3 and concomitant *TRAIL* downregulation (Fig. S5). We then transplanted these cells into NOG mice and evaluated their ability to form tumors without feeding the mice doxycycline.

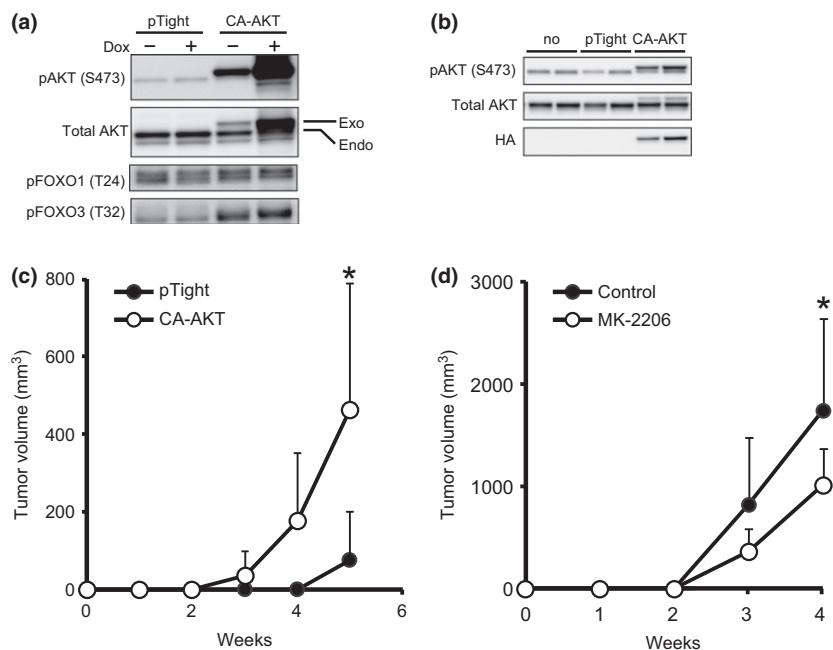
The CA-AKT-transduced cells showed rapid tumor development compared with the parental ST1 cells or control vector-transduced ST1 cells (Fig. 3c), indicating that the activation of AKT increased the tumorigenicity of the ST1 cells.

Next, we tested the effect of AKT suppression on tumor development. Treating NOG mice with the AKT inhibitor MK-2206 attenuated the tumor growth caused by ST1-N6 (Fig. 3d), supporting the role of AKT signaling in the tumorigenicity of ST1 cells. We did not observe any difference between the appearance of the MK-2206-treated group and that of the control group other than tumor growth. Collectively, these results suggested that enhanced AKT signaling may contribute to the tumorigenicity of ST1-N6 cells.

Decreased expression of negative regulators of the PI3K/AKT signaling axis in ST1-N6 cells. To explore the molecular mechanism(s) underlying the activation of AKT signaling in ST1-N6 cells, we first investigated the expression levels of PTEN in ST1-N6 and TL-Om1-N8 cells (Fig. S6a), as PTEN is known to negatively regulate AKT activation in many types of cells, including ATL cells. PTEN was undetectable even in the parental ST1 cells, suggesting that the deregulation of PTEN is not responsible for the aberrant activation of AKT in ST1-N6 cells. Interestingly, PTEN levels were decreased in TL-Om1-N8 cells compared with parental TL-Om1 cells, indicating that PTEN might be involved in the AKT activation of TL-Om1-N8 cells.

Next, to identify negative regulators other than PTEN that might be deregulated in ST1-N6 cells, we examined the gene expression profiles of protein phosphatase and lipid phosphatase family members by microarray analysis (Fig. S6b), because some of these enzymes have been reported to regulate AKT signaling. This analysis revealed several candidate suppressors whose expression levels were lower in the ST1-N6 cells than in the ST1 cells. Among them, we focused on INPP5D (also known as SHIP or SHIP-1) because its relationship to PI3K/AKT signaling was previously reported (see Discussion). ST1-N6 cells showed an attenuated expression of INPP5D at both the RNA and protein levels (Fig. 4a,b). The microarray analysis also showed decreased expression levels of

Fig. 3. Correlation between the tumorigenicity and protein kinase B (AKT) activation of ST1 cells. (a) Western blot showing the exogenously expressed constitutively active form of AKT (CA-AKT). Cells were first transduced with pRetroX-Tet-On Advanced retrovirus vector and then with control pRetroX-Tight-Pur (pTight) or a CA-AKT coding retrovirus vector. The cells were cultured with (+) or without (-) doxycycline (Dox) and analyzed by Western blot. The immunoblot was probed with an antibody to S473-phosphorylated AKT (pAKT) or total AKT. Exogenously expressed CA-AKT (Exo) and endogenous AKT (Endo) are indicated. (b) Western blot analysis of the developed tumors. Control ST1 cells (No) or the retrovirus-transduced cells described in (a) were injected into NOG mice, and the developed tumors were analyzed by Western blot. The blot probed with an anti-hemagglutinin antibody (HA) showed the expression of CA-AKT. (c) Tumor growth of control (pTight) or CA-AKT vector-transduced ST1 cells. Results from six injection sites were averaged. * $P < 0.05$. (d) Tumor growth by ST1-N6 cells in NOG mice treated with the AKT inhibitor MK-2206 or control vehicle (30% Captisol). Data shown are representative of two independent experiments. * $P < 0.05$.



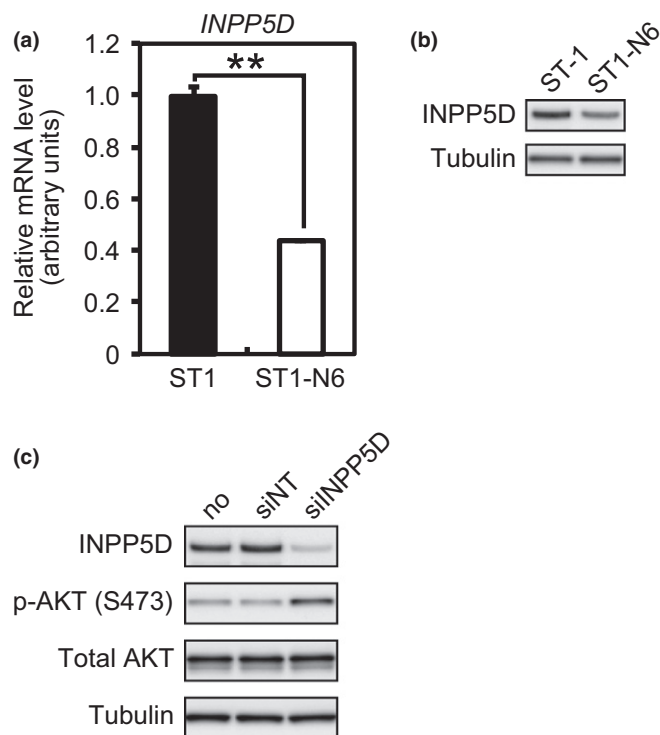


Fig. 4. Downregulation of inositol polyphosphate-5-phosphatase D (INPP5D) in ST1-N6 cells. The expression level of INPP5D was assayed by real time RT-PCR (a) and Western blotting (b). Results from three independent samples were averaged for the RT-PCR analysis. $**P < 0.01$. (c) Increased protein kinase B (AKT) phosphorylation in ST1 cells after siRNA-mediated gene knockdown of INPP5D. For the target gene, two siRNAs with different sequences were mixed (5 pmol, each siRNA) and introduced into ST1 cells (3×10^6 in 100 μ L) by electroporation. Cell lysates were prepared 48 h after electroporation and analyzed by Western blotting. No, cells without siRNA introduction; siNT, siRNA negative control.

protein or lipid phosphatases other than INPP5D, the significance of which is now under investigation.

To determine the physiological significance of the attenuated expression of INPP5D, we decreased its expression by siRNA-mediated gene knockdown and examined the phosphorylation levels of AKT. The knockdown of *INPP5D* (knockdown efficiency was 73%) caused an increase in AKT phosphorylation (Fig. 4c), suggesting that INPP5D may be involved in the activation of AKT signaling in ST1-N6 cells. The *INPP5D* expression level was similarly lower in TL-Om1-N8 cells than in TL-Om1 cells (Fig. S6c). Taken together, our findings indicate that deregulation of the suppressive machinery of AKT signaling is an important part of the process by which ATL cells become malignant through serial transplantation.

Discussion

Here we show that the serial xenotransplantation of ATL-derived cells into immunodeficient NOG mice results in the selection of highly tumorigenic cells. We established two highly tumorigenic sublines, ST1-N6 and TL-Om1-N8, from the ATL-derived ST1 and TL-Om1 cell lines, respectively. Notably, the *in vitro* growth rate of these sublines was almost the same as that of their parental cells. Based on a comparison with their parental cells, we discovered that AKT signaling was aberrant in these highly tumorigenic cells. Moreover, the tumorigenicity of ST1

cells was significantly enhanced by the transduction of a constitutively active form of AKT, further suggesting that AKT signaling has an important role in the tumorigenicity of ATL-derived cells. Although AKT signaling abnormalities in ATL cells have been reported previously,^(23–26) in this study we showed that the aberrant activation of AKT correlates well with the malignant phenotype of ATL-derived cells in xenotransplantation. In line with these observations, AKT activation in normal lymphocytes is reported to have an anti-apoptotic activity with little effect on the *in vitro* growth rate, resulting in lymphadenopathy and splenomegaly.⁽²⁷⁾

Little is known about the molecular mechanisms underlying the AKT abnormalities in ATL cells. Here we demonstrated that the upregulation of AKT signaling in ST1-N6 cells probably resulted from the downregulation of *INPP5D*. Inositol polyphosphate-5-phosphatase D hydrolyzes the 5'-phosphate of phosphatidylinositol (3,4,5)-trisphosphate and inositol 1,3,4,5-tetrakisphosphate,^(28–30) and is known to play a repressive role in AKT signaling.⁽³¹⁾ It has been shown that *Tax* induces the downregulation of INPP5D in peripheral blood T cells and Jurkat cells.⁽³²⁾ In the present study, however, *Tax* expression was decreased in ST1-N6 cells, indicating that a different INPP5D suppression mechanism occurs in the highly tumorigenic ATL-derived cells.

We also investigated how activated AKT regulates the tumorigenicity of ATL-derived cells following transplantation. Among the reported downstream proteins of AKT signaling,⁽³³⁾ we found that FOXO transcription factors, especially FOXO3, were phosphorylated and downregulated in ST1-N6 and TL-Om1-N8 cells. Experiments using the ectopic expression of constitutively active AKT further suggested that FOXO3 is one of the downstream targets of AKT in ST1 cells, although the functional significance of FOXOs in the tumorigenicity of ATL-derived cells remains untested. However, we did not detect the marked phosphorylation of other AKT target proteins, including p70 S6 kinase or glycogen synthase kinase 3 β (data not shown).

The NF- κ B pathway is also activated in ST1-N6 cells (Fig. S4b). Because NF- κ B signaling is known to participate in the malignancy of ATL, it is highly possible that this activation also contributes to the tumorigenicity of ST1-N6 cells. We are now investigating the molecular mechanisms by which the upregulation of NF- κ B signaling and its downstream targets may modulate the tumorigenicity of ST1-N6 cells. We have also examined the activation states of the ERK and JAK/STAT signaling pathways, but have not yet obtained evidence that these signaling molecules are upregulated in the highly tumorigenic cell lines.

Acknowledgments

The authors thank Dr. M. Ito (Central Institute for Experimental Animals) for providing the NOG mice, Dr. T. Kitamura (Tokyo University) for providing the Plat A cells, Dr. Y. Yamada (Nagasaki University) for providing the ST1 cells, Dr. W. Sellers (Harvard Medical School) for providing the plasmid pLNCX-Myr-HA-Akt1, and Dr. B. Sugden (University of Wisconsin) for providing the plasmid p1242 3-KB-L. This study was supported in part by Japan Society for the Promotion of Science KAKENHI grants to K.Y. (#24570142), S.I. (#26830087), and K.S. (#25290047).

Disclosure Statement

The authors have no conflict of interest.

Abbreviations

AKT	AKT8 virus oncogene cellular homolog
ATL	adult T-cell leukemia/lymphoma
CA-AKT	constitutively active human AKT
HA	hemagglutinin
HTLV-1	human T-cell lymphotropic virus-1

INPP5D	inositol polyphosphate-5-phosphatase D
NF- κ B	nuclear factor- κ B
NOG	NOD/SCID/IL-2R γ ^{null}
PI3K	phosphatidylinositol 3-kinase
PTEN	phosphatase and tensin homolog deleted on chromosome 10

References

- Yoshida M. Molecular approach to human leukemia: Isolation and characterization of the first human retrovirus HTLV-1 and its impact on tumorigenesis in Adult T-cell Leukemia. *Proc Jpn Acad Ser B Phys Biol Sci* 2010; **86**: 117–30.
- Matsuoka M, Jeang KT. Human T-cell leukaemia virus type 1 (HTLV-1) infectivity and cellular transformation. *Nat Rev Cancer* 2007; **7**: 270–80.
- Matsuoka M, Green PL. The HBZ gene, a key player in HTLV-1 pathogenesis. *Retrovirology* 2009; **6**: 71.
- Kfoury Y, Nasr R, Journo C, Mahieux R, Pique C, Bazarbachi A. The multifaceted oncoprotein Tax: Subcellular localization, posttranslational modifications, and NF- κ B activation. *Adv Cancer Res* 2012; **113**: 85–120.
- Yamagishi M, Watanabe T. Molecular hallmarks of adult T cell leukemia. *Front Microbiol* 2012; **3**: 334.
- Fidler IJ. Tumor heterogeneity and the biology of cancer invasion and metastasis. *Cancer Res* 1978; **38**: 2651–60.
- Woodruff MF. Cellular heterogeneity in tumours. *Br J Cancer* 1983; **47**: 589–94.
- Meacham CE, Morrison SJ. Tumour heterogeneity and cancer cell plasticity. *Nature* 2013; **501**: 328–37.
- Clarke MF, Dick JE, Dirks PB et al. Cancer stem cells—perspectives on current status and future directions: AACR workshop on cancer stem cells. *Cancer Res* 2006; **66**: 9339–44.
- Ito M, Hiramatsu H, Kobayashi K et al. NOD/SCID/IL-2R γ ^{null} mouse: an excellent recipient mouse model for engraftment of human cells. *Blood* 2002; **100**: 3175–82.
- Kimura O, Takahashi T, Ishii N et al. Characterization of the epithelial cell adhesion molecule (EpCAM)⁺ cell population in hepatocellular carcinoma cell lines. *Cancer Sci* 2010; **101**: 2145–55.
- Imai T, Tamai K, Oizumi S et al. CD271 defines a stem cell-like population in hypopharyngeal cancer. *PLoS ONE* 2013; **8**: e62002.
- Tamai K, Nakamura M, Mizuma M et al. Suppressive expression of CD274 increases tumorigenesis and cancer stem cell phenotypes in cholangiocarcinoma. *Cancer Sci* 2014; **105**: 667–74.
- Kobayashi S, Yamada-Okabe H, Suzuki M et al. LGR5-positive colon cancer stem cells interconvert with drug-resistant LGR5-negative cells and are capable of tumor reconstitution. *Stem Cells* 2012; **30**: 2631–44.
- Ramaswamy S, Nakamura N, Vazquez F et al. Regulation of G1 progression by the PTEN tumor suppressor protein is linked to inhibition of the phosphatidylinositol 3-kinase/AKT pathway. *Proc Natl Acad Sci USA* 1999; **96**: 2110–5.
- Mitchell T, Sugden B. Stimulation of NF- κ B-mediated transcription by mutant derivatives of the latent membrane protein of Epstein-Barr virus. *J Virol* 1995; **69**: 2968–76.
- Yamada Y, Sugahara K, Tsuruda K et al. Fas-resistance in ATL cell lines not associated with HTLV-1 or FAP-1 production. *Cancer Lett* 1999; **147**: 215–9.
- Sugamura K, Fujii M, Kannagi M, Sakitani M, Takeuchi M, Hinuma Y. Cell surface phenotypes and expression of viral antigens of various human cell lines carrying human T-cell leukemia virus. *Int J Cancer* 1984; **34**: 221–8.
- Fridman R, Benton G, Aranoutova I, Kleinman HK, Bonfil RD. Increased initiation and growth of tumor cell lines, cancer stem cells and biopsy material in mice using basement membrane matrix protein (Cultrex or Matrigel) co-injection. *Nat Protoc* 2012; **7**: 1138–44.
- Ou DL, Lee BS, Lin LI et al. Vertical blockade of the IGFR- PI3K/AKT /mTOR pathway for the treatment of hepatocellular carcinoma: The role of survivin. *Mol Cancer* 2014; **13**: 2.
- Fayard E, Xue G, Parcellier A, Bozulic L, Hemmings BA. Protein kinase B (PKB/AKT), a key mediator of the PI3K signaling pathway. *Curr Top Microbiol Immunol* 2010; **346**: 31–56.
- Vogt PK, Jiang H, Aoki M. Triple layer control: Phosphorylation, acetylation and ubiquitination of FOXO proteins. *Cell Cycle* 2005; **4**: 908–13.
- Jeong SJ, Pise-Masison CA, Radonovich MF, Park HU, Brady JN. Activated AKT regulates NF- κ B activation, p53 inhibition and cell survival in HTLV-1-transformed cells. *Oncogene* 2005; **24**: 6719–28.
- Fukuda R, Hayashi A, Utsunomiya A et al. Alteration of phosphatidylinositol 3-kinase cascade in the multilobulated nuclear formation of adult T cell leukemia/lymphoma (ATLL). *Proc Natl Acad Sci USA* 2005; **102**: 15213–8.
- Bellon M, Nicot C. Central role of PI3K in transcriptional activation of hTERT in HTLV-1-infected cells. *Blood* 2008; **112**: 2946–55.
- Nakahata S, Ichikawa T, Maneesaay P et al. Loss of NDRG2 expression activates PI3K-AKT signalling via PTEN phosphorylation in ATLL and other cancers. *Nat Commun* 2014; **5**: 3393.
- Parsons MJ, Jones RG, Tsao MS, Oudermatt B, Ohashi PS, Woodgett JR. Expression of active protein kinase B in T cells perturbs both T and B cell homeostasis and promotes inflammation. *J Immunol* 2001; **167**: 42–8.
- Damen JE, Liu L, Rosten P et al. The 145-kDa protein induced to associate with Shc by multiple cytokines is an inositol tetrakisphosphate and phosphatidylinositol 3,4,5-triphosphate 5-phosphatase. *Proc Natl Acad Sci USA* 1996; **93**: 1689–93.
- Lioubin MN, Algate PA, Tsai S, Carlberg K, Aebersold A, Rohrschneider LR. P150Ship, a signal transduction molecule with inositol polyphosphate-5-phosphatase activity. *Genes Dev* 1996; **10**: 1084–95.
- Chacko GW, Tridandapani S, Damen JE, Liu L, Krystal G, Coggeshall KM. Negative signaling in B lymphocytes induces tyrosine phosphorylation of the 145-kDa inositol polyphosphate 5-phosphatase. *SHIP. J Immunol* 1996; **157**: 2234–8.
- Aman MJ, Lamkin TD, Okada H, Kurosaki T, Ravichandran KS. The inositol phosphatase SHIP inhibits AKT/PKB activation in B cells. *J Biol Chem* 1998; **273**: 33922–8.
- Fukuda RI, Tsuchiya K, Suzuki K et al. HTLV-1 tax regulates the cellular proliferation through the down-regulation of PIP3-phosphatase expressions via the NF- κ B pathway. *Int J Biochem Mol Biol* 2012; **3**: 95–104.
- Manning BD, Cantley LC. AKT/PKB signaling: Navigating downstream. *Cell* 2007; **129**: 1261–74.

Supporting Information

Additional Supporting Information may be found online in the supporting information tab for this article:

Fig. S1. Times for the development of palpable tumors in NOG mice.

Fig. S2. Tumor growth from TL-Om1 and TL-Om1-N8 cells in NOG mice.

Fig. S3. Growth properties of ST1-N6 and TL-Om1-N8 cells *in vitro*.

Fig. S4. Expression levels of viral oncogenes and activation of nuclear factor- κ B (NF- κ B) signaling in ST1-N6 cells.

Fig. S5. AKT-dependent downregulation of FOXO-target gene TRAIL in CA-AKT expressing cells.

Fig. S6. Decreased expression of molecules regulating the AKT signal.

Table S1. Oligonucleotide sequences for quantitative RT-PCR (qRT-PCR) and for siRNA-mediated gene knockdown (siRNA).